第32卷第12期 焊 接 学 报 Vol. 32 No. 12
2011年12月 TRANSACTIONS OF THE CHINA WELDING INSTITUTION December 2011

PCBN磨粒/石墨/CuSnTi合金复合块界面微观结构

张 斌， 丁文锋， 徐九华， 陈珍珍*
(南京航空航天大学 机电学院，南京 210016)

张 斌

摘 要：在加热温度920 ℃和保温时间30 min工艺下，进行铜锡钛(Cu-Sn-Ti)合金与石墨颗粒、聚晶立方氮化硼(PCBN)磨粒的烧结试验. 通过三点抗弯试验测试了烧结试样的强度，并使用扫描电镜、能谱仪、X射线衍射仪检测了复合块的断口形貌与物相组成. 结果表明，石墨质量分数为5%～15%时烧结试样的抗弯强度达91 MPa以上，高于陶瓷砂轮工作层强度；试样烧结过程中发生了元素扩散，在结合界面处形成了化合物，实现了PCBN磨粒与Cu-Sn-Ti合金之间的化学结合；由于复合块对PCBN磨粒的牢固把持作用，抗弯试验过程中复合块内部的PCBN磨粒发生沿晶断裂.

关键词：聚晶立方氮化硼磨粒；铜锡钛合金；抗弯强度；界面微观结构
中图分类号：TG401 **文献标识码**：A **文章编号**：0253－360X(2011)12－0063－03

0 序 言

立方氮化硼(CBN)具有硬度高和热稳定性好的优异性能. 利用CBN制作的超硬磨料磨具，特别适合于钛合金、高温合金等高强韧性难加工金属材料的高性能磨削加工[1,2]. 但钎焊CBN砂轮在磨削过程中，由于工件与砂轮之间强烈的力-热耦合作用，使得CBN磨粒发生磨耗磨损，影响CBN砂轮的性能发挥和研制进程.

聚晶立方氮化硼(PCBN)磨粒是由CBN微晶磨粒和一定比例的陶瓷粘结剂(如AlN)在高温高压下烧结而成的. 如果使用PCBN磨粒制作砂轮，在磨削的过程中，一旦磨粒磨钝，在逐渐增大的磨削力作用下，AlN粘结剂与CBN微晶磨粒结合面发生脱粘，造成磨钝的CBN微晶颗粒脱落，可使内部的CBN微晶磨粒不断裸露出来继续参与磨削. PCBN磨粒这种自锐特性使得砂轮可始终维持在锋利的状态，不会导致磨削力和磨削温度的急剧增加，同时可以减少砂轮修整次数，显著提高效率和加工质量[3]. 为此文中提出通过高温活性烧结的方法使PCBN磨粒与金属结合剂之间形成牢固的化学结合，确保PCBN优异磨削潜能充分发挥.

收稿日期：2010－09－25
基金项目：国家重点基础研究发展计划资助项目(2009CB724403)；国家自然科学基金资助项目(51005116)；江苏省自然科学基金资助项目(BK2010496)；中国博士后科学基金资助项目(20110490167)
* 参加该项目研究工作的还有苏宏华，傅玉灿

1 试验方法

1.1 试样制备

试验所用材料为PCBN磨粒、Cu-Sn-Ti合金和石墨颗粒. PCBN的粒度为106～125 μm，以AlN为粘结剂，PCBN磨粒中的CBN微晶磨粒与AlN的结合形貌如图1所示. 文中制作了三组砂轮复合块，每组试样的组元配比见表1.

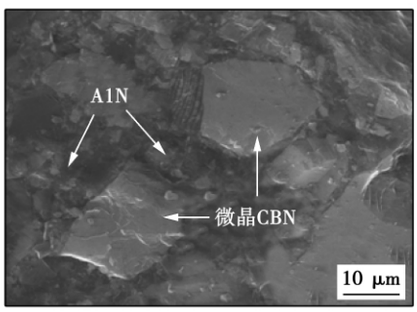

图1 原始PCBN磨粒微观形貌
Fig. 1 Micrograph of original PCBN grain

表1 复合块原料及其含量(质量分数，%)
Table 1 Raw material and corresponding mass fractions of sintering composites

复合块	PCBN	石墨	铜锡钛
第一组	20	5	75
第二组	20	10	70
第三组	20	15	65

烧结过程中，由于熔融 Cu-Sn-Ti 合金的流失会使得整个试样塌陷，不能保持住压制好的形状，而添加石墨颗粒则可阻碍液相合金的流动，有助于试样烧结成形.

对 PCBN 磨粒进行去油、去污处理；用 Adventurer 型分析天平称量原料；将成形剂加入称量好的原料中搅拌均匀后烘干，再将其填装进模具中，在粉末压片机上压制成形；将压制成形的节块放入真空炉内以加热温度 920 ℃和保温时间 30 min 的工艺进行烧结，最后随炉冷却至室温.

1.2 试验及分析方法

使用 SANS 型万能材料试验机对复合块进行三点抗弯强度测试，支点跨距为 25 mm，试验机加载速度 0.5 mm/min. 利用 Quanta200 型扫描电镜、EDAX 能谱仪、XD-3A 型 X 射线衍射仪分析复合块断口的界面微结构与物相组成.

2 试验结果与讨论

2.1 复合块的抗弯强度

图 2 显示了石墨质量分数为 5% 时复合块的载荷力—位移变化曲线. 可以看出，在试验机压头加载的初期阶段，复合块所受的载荷力随着位移的增加呈非常缓慢变化的曲线上升；随着压头位移的继续增加，载荷力呈近似直线上升，直到载荷力达到最大值 1 200 N 左右时复合块断裂，由此获得复合块的断裂强度.

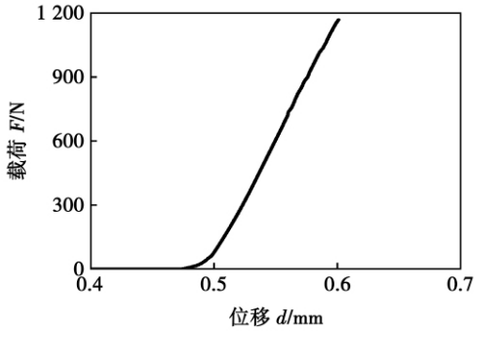

图 2 三点抗弯试验的力—位移曲线

Fig. 2 Force-displacement curve of three-point bending experiments

图 3 为石墨含量对复合试样抗弯强度的影响. 很明显，复合块的抗弯强度随着石墨含量的增加逐渐下降. 当石墨质量分数为 5% 时，试样的抗弯强度最大，为 136 MPa；当石墨质量分数增加到 15% 时，试样的抗弯强度下降到 91 MPa. 总体而言，当石墨质量分数为 5% ~ 15% 时，复合块的抗弯强度均高于传统陶瓷砂轮工作层的抗弯强度. 考虑到试样活性烧结反应机理的相似性，文中以下对石墨质量分数为 5 % 的复合块的烧结界面微结构与形成机理进行了讨论.

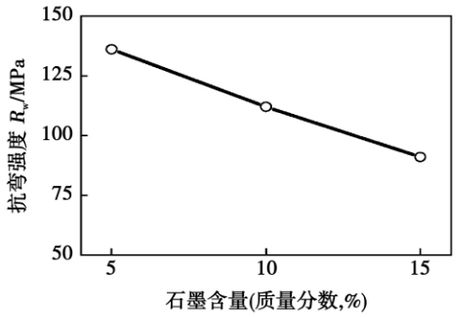

图 3 石墨对复合块抗弯强度的影响

Fig. 3 Effect of graphite particles on bending strength of sintering composites

2.2 复合块断口形貌

图 4 为复合块断口形貌，从中可以发现 PCBN 磨粒、Cu-Sn-Ti 合金和部分孔隙. 其中 PCBN 磨粒发生断裂，说明 Cu-Sn-Ti 合金已牢固把持住了 PCBN 磨粒. 复合块中的孔隙是在熔融状态的 Cu-Sn-Ti 合金从烧结温度下降到室温过程中，随着合金冷却收缩而形成的.

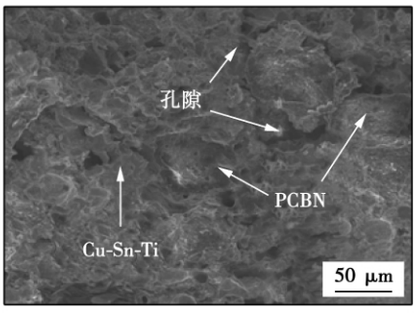

图 4 复合块断口形貌

Fig. 4 Micrograph of fracture surface of sintering composites

图 5 为 PCBN 复合块断口上石墨颗粒与 Cu-Sn-Ti 合金的结合面. 很明显，石墨呈鳞片状，侧面局部位置出现台阶，证实了石墨存在层状解理面结构. 石墨的线膨胀系数远小于 Cu-Sn-Ti 合金. 因此当试样从烧结温度 920 ℃逐渐冷却至室温时，由于线膨胀系数的差异，合金与石墨的结合界面会产生一定的应力. 当复合块断裂时的微裂纹扩展至合金与石

墨的结合面，应力的释放会加速裂纹的扩展，同时石墨在受力的情况下也会沿着解理面解理. 这些都会导致复合块力学性能下降. 所以随着石墨含量增加，复合块的抗弯强度呈下降的趋势.

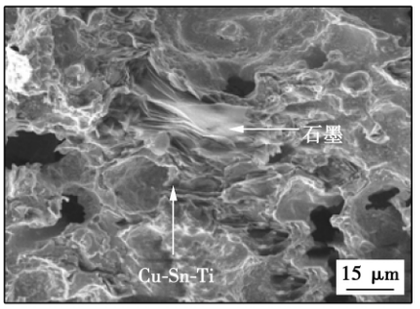

图 5　石墨与合金结合界面

Fig. 5　Microstructure of interface between graphite particle and Cu-Sn-Ti alloy

2.3　PCBN 磨粒与 Cu-Sn-Ti 合金界面微观结构

图 6 为 PCBN 磨粒与 Cu-Sn-Ti 合金结合界面的微结构与元素分布. 由图 6a 可以看出，虽然 Cu-Sn-Ti 合金层中存在部分孔隙，但 PCBN 磨粒与合金的结合界面致密，在磨粒与合金结合界面处没有明显的孔隙. PCBN 磨粒的断口表面上密布着 CBN 微晶磨粒.

图 6b 显示了 PCBN 磨粒与 Cu-Sn-Ti 合金结合界面的元素分布特征. 很明显，合金中活性元素 Ti 在结合界面处存在着波峰，说明 Ti 元素在结合面呈现富集状态. 元素 B，N 在结合界面处呈现递增趋势，这说明元素 Ti，B，N 在烧结过程中发生了扩散偏聚. 结合面的右边存在 Al 元素主要来源于 PCBN 磨粒中的粘结剂 AlN.

为了证实结合面处形成了化合物，对复合块断口进行 X 射线衍射分析，结果如图 6c 所示. 总体而言，烧结后复合块的物相主要是 C(石墨)，CBN，AlN 和 Cu-Sn 合金之间的相关产物，同时在烧结过程中还生成了 TiN，TiB_2，TiC，$TiAl_3$ 等化合物.

化合物 TiN 的生成过程比较复杂，大致由两部分组成[8]：Ti 元素与 CBN 微晶磨粒反应生成；Ti 元素与 AlN 反应生成. 粘结剂与活性元素 Ti 可能生成 $TiAl_3$，Ti_3Al[9]，但在此试验中，由于 Ti_3Al 非常少而未发现其衍射峰.

$TiAl_3$ 的反应方程式可表示为

$$4Ti + 3AlN = TiAl_3 + 3TiN \quad (1)$$

以上分析 Cu-Sn-Ti 合金在高温下熔化成液态，浸润并吸附在磨粒表面 PCBN，与其发生化学反应生成化合物，形成化学结合，提高了界面结合强度.

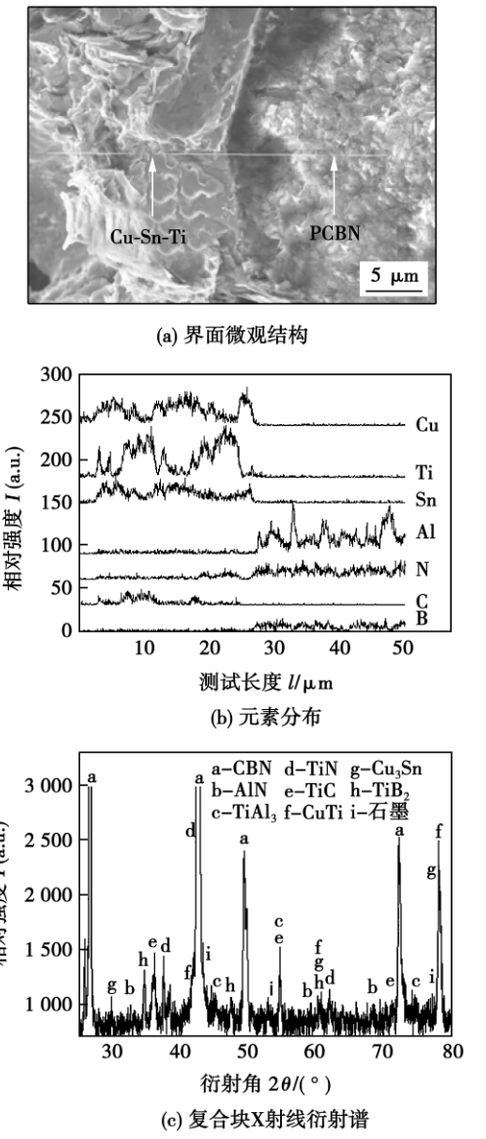

图 6　PCBN 磨粒与 Cu-Sn-Ti 合金结合界面

Fig. 6　Joining interface between PCBN grain and Cu-Sn-Ti alloy

PCBN 磨粒的断裂韧度为 6.8 $MPa/m^{1/2}$，单晶 CBN 磨粒的断裂韧度为 2.8 $MPa/m^{1/2}$[6]，相比于单晶 CBN 磨粒，PCBN 磨粒提高了抵抗裂纹扩展的能力. 试样受载断裂时，由于复合块对 PCBN 磨粒的把持作用已高于 PCBN 磨粒自身强度，所以 PCBN 磨粒即使断裂，也未被连根拔出，而是磨粒中的 AlN 粘结剂与 CBN 微晶磨粒结合面发生脱粘，裂纹沿着 CBN 微晶磨粒扩展，形成沿晶断裂.

图 7 为 PCBN 磨粒断口形貌，可以看到 PCBN 磨粒断口表面相对平直，没有出现明显的凹坑与突起，同时部分 CBN 微晶磨粒上粘结着 AlN. 说明 PCBN 磨粒断裂时不会大块脱落，而是单个或局部

[下转第 69 页]

5　结　　论

（1）对 SYSWELD 软件进行了二次开发，利用现有单一热源模式计算了 K-PAW 的焊接温度场，焊接熔合线与实际的熔合线有较大差异.

（2）根据 K-PAW 的焊缝形状特点以及沿工件厚度方向体积分布的特点，找出了适合于 K-PAW 焊接的组合式体积热源作用模式，即，沿板厚方向，工件的上部采用双椭球体热源，下部为中心轴热流峰值线性递增的圆柱体热源.

（3）将“双椭球体 + 峰值线性递增圆柱体”组合式热源应用于 SYSWELD 软件与 K-PAW 焊接热过程有限元模型，计算了 6 mm 厚不锈钢板 K-PAW 焊接温度场以及焊缝形状尺寸，计算结果与试验结果吻合良好.

参考文献：

[1] Hu Qingxian，Wu Chuansong，Zhang Yuming. Experimental determination of the weld penetration evolution in keyhole plasma arc welding [J]. China Welding，2007，16(1)：6－8.

[2] Hu Qingxian，Wu Chuansong，Zhang Yuming. Finite element analysis of keyhole plasma arc welding based on an adaptive heat source mode [J]. China Welding，2007，16(2)：55－58.

[3] 武传松. 焊接热过程与熔池形态 [M]. 北京：机械工业出版社，2007.

[4] 胡庆贤. 穿孔等离子弧焊接温度场的有限元分析 [D]. 济南：山东大学，2007.

[5] 高洪明. 双面电弧焊接熔池温度场与流场数值模拟及其机理探讨 [D]. 哈尔滨：哈尔滨工业大学，2001.

作者简介：胡庆贤，男，1976 年出生，博士，讲师. 主要从事焊接数值模拟与仿真方面的科研和教学工作. 发表论文 20 余篇. Email：huqingxian@126.com.

[上接第 65 页]

的 CBN 微晶磨粒逐步脱落. 由此可以认为，PCBN 磨粒在磨削过程中可发生微刃破碎，从而有利于更好地发挥砂轮的自锐特性.

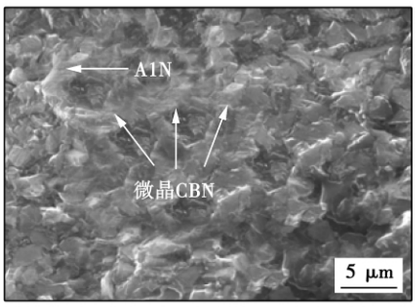

图 7　复合块中 PCBN 磨粒断口形貌

Fig. 7　Micrograph of fracture surface of PCBN grain within sintering composite

3　结　　论

（1）石墨质量分数为 5% ～15% 时 PCBN 复合块的抗弯强度达到 91 MPa 以上，高于传统陶瓷砂轮工作层的强度.

（2）PCBN 磨粒与 Cu-Sn-Ti 合金在烧结过程中发生了界面元素扩散，形成 TiN，TiB_2 等化合物，实现了 PCBN 磨粒与合金之间的牢固结合.

（3）复合块对 PCBN 磨粒的把持作用高于 PCBN 磨粒自身强度，使得复合块断裂的主要形式为 PCBN 磨粒内部的沿晶断裂.

参考文献：

[1] Chattopadhyay A K，Hintermann H E. On brazing of cubic boron nitride abrasive crystals to steel substrate with alloys containing Cr or Ti [J]. Journal of Materials Science，1993，28：5887－5893.

[2] Sumiya H，Uesaka S，Satoh S. Mechanical properties of high purity polycrystalline CBN synthesized by direct conversion sintering method [J]. Journal of Materials Science，2000，35(5)：1181－1186.

[3] Sunarto，Ichida Y. Creep feed profile grinding of Ni-based superalloys with ultrafine-polycrystalline CBN abrasive grits [J]. Precision Engineering，2001，25(4)：274－283.

[4] Ding W F，Xu J H，Fu Y C，*et al*. Interfacial reaction between cubic boron nitride and Ti during active brazing [J]. Journal of Materials Engineering and Performance，2007，15(3)：365－369.

[5] El-Sayed M H，Naka M，Schuster J C. Interfacial structure and reaction mechanism of AlN/Ti joints [J]. Journal of Materials Science，1997，32(10)：2715－2721.

[6] Develyn M P，Taniguchi T. Elastic properties of translucent polycrystalline cubic boron nitride as characterized by the dynamic resonance method [J]. Diamond and Related Materials，1999，8(8/9)：1522－1526.

作者简介：张　斌，男，1987 年出生，硕士生. 主要从事高性能超硬磨料工具制作与性能评价工作. Email：graduatezhang@126.com

通讯作者：丁文锋，男，博士，副教授. Email：dingwf2000@vip.163.com

Through comparing the simulation results and experimental measurements, the prediction accuracy of the developed thermo-elastic-plastic FEM based on Quick Welder was verified. Meanwhile, the influence of welding sequence on the residual stress distribution was clarified using numerical simulation method. The results show that both transverse residual stress and longitudinal residual stress were significantly affected by deposition sequence. The deposition sequence not only largely changes the peak values of residual stress, but also alters the shape of residual stress distribution.

Key words: numerical simulation; non-linear analysis; welding residual stress; welding sequence

Nanoindentation measurement of Sn-Cu-Ni joint WANG Jianxin, LAI Zhongmin, SUN Dandan (Province Key Lab of Advanced Welding Technology, Jiangsu University of Science and Technology, Zhenjiang 212003, China). p 59 - 62

Abstract: In order to study the effect of intermetallic compound on mechanical properties of joint, the elastic modulus and hardness of intermetallic compounds were analyzed by nanoindentation method, and the creep strain rate sensitivity of solder matrix was obtained by Mayo-Nix method. From the physical analysis of nanoindentation curves, the elastic modulu of $(Cu, Ni)_6Sn_5$ in Sn-Cu-Ni joints is 113.2 GPa ± 4.8 GPa, while the hardness is 5.59 GPa ± 0.32 GPa. It is found that intermetallic compounds are the key factors in the reliability of lead-free joints, due to the big contrasts between mechanical properties of intermetallic compounds and solder matrix. The creep strain rate sensitivities of Sn-Cu-Ni, Sn-Cu-Ni-0.05Ce and Sn-Pb solder matrix are 0.1286, 0.1248, and 0.1832, and the creep stress exponents are 7.7760, 8.0128, and 5.4585, respectively, which indicate the improvement in creep resistance of Sn-Cu-Ni joints due to Ce addition.

Key words: lead-free solder; nanoindentation; elastic modulu; creep strain rate sensitivity

Interfacial microstructure of sintering composites of PCBN grains-graphite particles-CuSnTi alloy ZHANG Bin, DING Wenfeng, XU Jiuhua, CHEN Zhenzhen, SU Honghua, FU Yucan (College of Mechanical and Electrical Engineering, Nanjing University of Aeronautics and Astronautics, Nanjing 210016, China). p 63 - 65, 69

Abstract: Sintering experiments of Cu-Sn-Ti alloy, polycrystalline cubic boron nitride (PCBN) abrasive grains and graphite particles were carried out at the heating temperature of 920 ℃ with the dwell time of 30 min. The strength of sintering bulks was measured by means of the three-point bending experiments. The interfacial microstructure and the phases of the sintering bulks were characterized using scanning electron microscope (SEM), energy dispersion spectrometer (EDS) and X-ray diffraction (XRD). The results reveal that in the case of the graphite content of 5 ~ 15 wt%, the bending strength of the composite bulks is above 91 MPa, which is much higher than that of the bulk strength of the vitrified grinding wheels. The elemental diffusion behavior has taken place across the joining interface between PCBN grains and Cu-Sn-Ti alloy in the sintering process. The compounds were formed, therefore, the PCBN grains were bonded firmly. Under such condition, the breakage of the PCBN grains has played the most important role in the fracture of the composite bulks. In particular, the breakage mode of the PCBN grains is the intergranular fracture.

Key words: PCBN abrasive grains; Cu-Sn-Ti alloy; bending strength; interfacial microstructure

Finite element analysis of temperature field during keyhole-plasma arc welding using SYSWELD software HU Qingxian[1], WANG Yanhui[1], YAO Qingjun[2], WANG Shunyao[1] (1. Provincial Key Lab of Advanced Welding Technology, Jiangsu University of Science and Technology, Zhenjiang 212003, China; 2. Jiangsu Province Special Equipment Safety Supervision Inspection Institute, Yangzhou Branch, Yangzhou 225003, China). p 66 - 69

Abstract: Considering the weld geometric characters of keyhole plasma arc welding (K-PAW), a suitable and adaptive combined heat source for numerical simulation is developed, i.e. at the transverse cross-section and along the workpiece thickness direction, the double-ellipsoidal volumetric heat source acts at upper part of the workpiece while a linearly-increased peak value of heat flux in gaussian cylinder mode exerts at lower part of the workpiece. Based on the developed adaptive combined heat source model, the welding temperature field of 6 mm thickness stainless steel is simulated by SYSWELD. The predicted weld geometry and fusion line locus at cross-section are in good agreement with the experimental measurement. This demonstrates the suitability of the combined volumetric heat source mode.

Key words: keyhole plasma arc welding; temperature field; combined volumetric heat source; finite element analysis

Study on ultrasonic stir hybrid welding of aluminum alloy HE Diqiu, LI Jian, LI Donghui, LIANG Jianzhang (State Key Laboratory of High-performance Complex Manufacturing, Central South University, Changsha 410083, China). p 70 - 72, 108

Abstract: Friction stir welding (FSW) of aluminum alloy usually results in a special "funnel shaped" temperature field, which makes obvious difference of microstructure properties in the direction of weld seams. In order to get better properties of welded joints, ultrasonic stir hybrid welding technology has been put forward in this paper, which concentrates the ultrasonic energy in deep weld seams through the stirring pin. Thickness of 2.5 mm 2219 aluminum alloy sheets has been adopted and welded by the two technologies mentioned above in this experiment, microstructure and mechanical properties of weld are analyzed and compared as well. Result shows that the weld joints of 2219 aluminum welded by the two technologies are both with good appearance and defect-free in the inner, and ultrasonic stir hybrid welding obviously has better mechanical properties.

Key words: ultrasonic stir hybrid welding; friction stir welding; 2219 aluminum alloy

Effect of Nd addition on microstructure and mechanical property of Sn3.8Ag0.7Cu solder joint GAO Lili, XUE Songbai, WANG Bo (College of Materials Science and Technology, Nanjing University of Aeronautics and Astronautics, Nanjing 210016, China). p 73 - 76

Abstract: The effects of Nd addition(0, 0.05, 0.5wt%) on the microstructure and shear strength of SAC solder joint under as-reflowed and 150 ℃ isothermal-aging process were investigated. Experimental results showed that Nd addition can obviously improve the shear strength and microstructure of the SAC solder joints. The growth rate of the SAC/Cu interfacial layer as